Electronic Supplementary Material (ESI) for Journal of Materials Chemistry C.

Bismuthene-based multifunctional all-optical phase and intensity modulator enabled by photothermal effect

Yunzheng Wang, [a] Weichun Huang, [a] Jinlai Zhao, [b] Hao Huang, [a] Cong Wang, [c] Feng Zhang, [a] Jie Liu, [c] Jianqing Li, [b] Meng Zhang [d] and Han Zhang*[a]

[a.] *International Collaborative Laboratory of 2D Materials for Optoelectronics Science and Technology of Ministry of Education, College of Optoelectronic Engineering, Shenzhen University, Shenzhen 518060, China. E-mail: hzhang@szu.edu.cn*

[b.] *Faculty of Information Technology, Macau University of Science and Technology, Macao, P. R. China.*

[c.] *Shandong Provincial Key Laboratory of Optics and Photonic Device, School of Physics and Electronics, Shandong Normal University, Jinan 250014, China.*

[d.] *School of Electronic and Information Engineering, Beihang University, Beijing, 100191, China.*

S1. Material Preparation

Few-layer bismuth quantum dots (BiQDs) were facilely fabricated using a liquid-phase exfoliation method. Firstly, bismuth (Bi) powder (Aladdin, 99.9% metals basis, ≥ 200 meshes) was mixed with pure 1-Methyl-2-pyrrolidinone (NMP) with a concentration of 10 mg/mL. The Bi/NMP slurry was successively sonicated in a probe sonication device (Bilon, BILON-1800Y) for 12 h, then diluted into 0.1 mg/mL, and continued to be sonicated in a built-in cooling water equipment for 48 h. After that, a centrifugation process was conducted at 7,000 rpm and the supernatant was decanted gently to another tube for further centrifugation at 18,000 rpm for 30 min to achieve the targeted precipitate of BiQDs. To facilitate subsequent optical deposition process, volatile isopropyl alcohol (IPA) took the place of low volatile NMP in the process of solvent exchange.

S2. Fabrication of BiQDs-deposited microfiber

First, a single mode fiber was heated by an alcohol lamp and tapered into a microfiber with a diameter of ~ 8 um. Then, some BiQDs/IPA suspension was dropped to the surface of microfiber and a laser beam was injected. The BiQDs were effectively attracted to the side face of the microfiber by strong evanescent field. At the same time, the deposition process was monitored by a power meter and an optical microscope. Finally, when the insertion loss of BiQDs-deposited microfiber reached about 5~8 dB, the pump source was turned off and the deposition process was stopped.

S3. Experimental setup of all-optical phase modulator

The proposed all-optical phase modulator mainly consisted of a fiber-type Michelson interferometer (MI) which had a modulation arm (the upper arm in Fig. 3) and a reference arm (the lower arm in Fig. 3). An amplified spontaneous emission (ASE) source of 1550 nm and a laser diode of 980 nm served as signal source and pump source to supply broadband signal light and intense pump light, respectively. The signal light and the pump light were combined by a wavelength division multiplexer (WDM) and injected into MI through an optical coupler (OC). Because of wavelength dependence, the intensity splitting ratio of the OC was measured to be 50:50 and 90:10 at 1550 nm and 980 nm, respectively. The 90% port of OC was spliced with the modulation arm for high absorption efficiency of pump light. In modulation arm, a BiQDs-deposited microfiber was inserted to absorb the pump light and change the phase of signal light through thermo-optic effect. In reference arm, a variable optical attenuator (VOA) was contained to balance two signal lights of MI to achieve optimal interferometric contrast. In both arms, two identical Faraday rotation mirrors (FRM1 and FRM2) were used to reflect the signal light back. At the same time, FRMs could make sure that the reflected signal lights always have the same polarization state in position of OC to keep the optimal interferometric condition, regardless of ambient temperature perturbation and external mechanical vibration[22]. To prevent the reverse transmission light from damaging the light sources, an optical isolator was inserted between WDM and OC to block it. The interferometric spectrum of MI was exported from the fourth port of OC and monitored by an optical spectrum analyzer (Yokokawa, AQ6370D).

S4. The interferometric spectra obtained at different pump power.

Due to the saturable absorption of BiQDs, the interferometric contrast gradually reduces with the increase of the pump power. Fig. S1 shows typical interferometric spectra obtained at pump power of 0 mW and 420 mW. It can be easily observed that the interferometric contrast reduces from 25 dB to 9.3 dB.

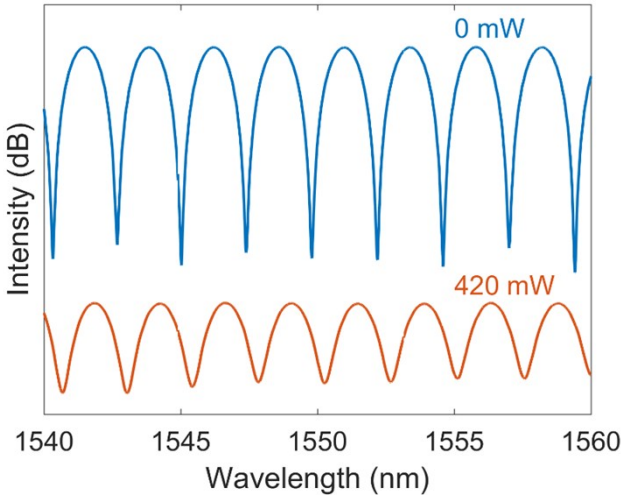

Fig. S1. Typical interferometric spectra measured at pump power of 0 mW and 420 mW.

S5. Influence of pump power on the transmittance of the BiQDs-deposited microfiber.

From Equation 1, the interferometric contrast of the interferometric spectrum can be derived as

$$C = \frac{I_1 + I_2 + 2\sqrt{I_1 I_2}}{I_1 + I_2 - 2\sqrt{I_1 I_2}}. \tag{S1}$$

where, I_1 and I_2 are the intensity of the signal lights reflected to OC in the modulation arm and the reference arm, respectively. Due to the saturable absorption of BiQDs, the transmittance of the BiQDs-deposited microfiber becomes larger with the increase of the pump power. Then the interferometric contrast is equal to

$$C' = \frac{I_1' + I_2' + 2\sqrt{I_1' I_2'}}{I_1' + I_2' - 2\sqrt{I_1' I_2'}}. \tag{S2}$$

Here, $I_2' = I_2$, because of no influence of pump power on the reference arm. According to experimental results, C and C' are 25 dB and 9.3 dB at pump power of 0 mW and 420 mW, respectively. So, it is reasonable to assume $I_1 \approx I_2$, and then $I_1' = 4.17 \times I_1$ can be obtained. Therefore, the transmittance at pump power of 420 mW is about twice than that without pump light in view of the fact that the signal light propagates through the BiQDs-deposited microfiber two times.

S6. Experimental setup of wavelength-tuning fiber laser

The fiber laser consisted of a WDM where 980 nm laser beam emitted from LD1 was guided into the fiber laser for population inversion, a piece of Erbium-doped fiber (EDF), an ISO to make sure the unidirectional operation, an OC that extracted some laser power from its 10% port, and the proposed all-optical phase modulator (AOM) whose spectral properties were controlled by another 980 nm laser diode (LD2). The output laser was further monitored by an OSA.

S7. Experimental setup of all-optical intensity modulator

Different from all-optical phase modulator shown in Figure 3, here a continuous-wave distributed feedback (DFB) laser instead of ASE source served as the signal source to supply narrowband signal light and the 980 nm LD was externally modulated by a computer to emit square-wave pump light with tunable

power and frequency. Additionally, the output signal light was detected by a photodetector and monitored by an oscilloscope.

S8. Theoretical simulation of the dependence of signal waveforms on the maximal phase shift.

Starting from Equation 3, if the wavelength of DFB light is equal to the valley wavelength of the interferometric spectrum, the relationship between the output signal intensity and the phase shift can be simplified as

$$I_{out}(\varphi_s)=\frac{1}{2}\left[1\text{-}\cos(\varphi_s)\right], \tag{S3}$$

where, I_{out} is the normalized intensity of output signal light, φ_S is the phase shift. Due to the hysteresis effect of the heat generation and dissipation, the response of the output signal light is always slower than the change of the pump light. Assuming the time-dependent phase shift is $\varphi_S(t)$, the output signal intensity can be written as

$$I_{out}(t)=\frac{1}{2}\left[1\text{-}\cos(\varphi_s(t))\right]. \tag{S4}$$

When the maximal phase shift $\varphi_{S,\ max}$ is equal to π rad, the rising edge of the normalized signal waveform can be fitted by the following exponential function

$$I_{out}(t)=1\text{-}e^{-t/t_r}, \tag{S5}$$

where, t_r is the time constant of the rising edge. By equating Equation S4 with Equation S5, we can achieve the analytic solution of $\varphi_S(t)$ as

$$\varphi_s(t)=\cos^{-1}\left(2e^{-t/t_r}-1\right). \tag{S6}$$

In practice, whatever the pump power is, the variation trend of the phase shift should meet this analytic solution. Therefore, Equation S6 can be generalized to arbitrary value of $\varphi_{S,\ max}$ as

$$\varphi_s(t)=\frac{\varphi_{s,\max}}{\pi}\cos^{-1}\left(2e^{-t/t_r}-1\right). \tag{S7}$$

Similarly, the time-dependent phase shift for the falling edge can be calculated as

$$\varphi_s(t)=\frac{\varphi_{s,\max}}{\pi}\cos^{-1}\left(1-2e^{-t/t_f}\right), \tag{S8}$$

where, t_f is the time constant of the falling edge. Using Equation S5, S7 and S8, the signal waveforms in Figure 6d can be theoretically simulated by selecting proper time constants for two edges.

In experiment, we also observe the condition that the $\varphi_{S,\ max}/\pi$ is not an integer. **Fig. S2** shows the measured signal waveform and corresponding simulation curve. From simulation, it can be derived that $\varphi_{S,\ max}=2.35\ \pi$.

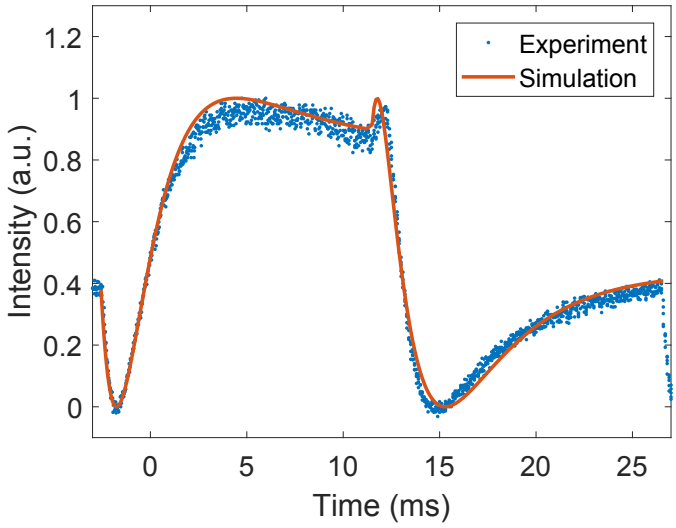

Fig. S2. Measured signal waveform and simulation curve at $\varphi_{S,\ max}=2.35\ \pi$.